Effect of electron beam irradiation on the interphase boundary between crystalline Al and amorphous Al_2O_3

2001 J. Phys.: Condens. Matter 13 8475

(http://iopscience.iop.org/0953-8984/13/37/304)

INSTITUTE OF PHYSICS PUBLISHING JOURNAL OF PHYSICS: CONDENSED MATTER

J. Phys.: Condens. Matter **13** (2001) 8475–8479 PII: S0953-8984(01)25605-7

Effect of electron beam irradiation on the interphase boundary between crystalline Al and amorphous Al_2O_3

Z Q Yang[1], L L He, Z X Jin and H Q Ye

Laboratory of Atomic Imaging of Solids, Institute of Metal Research, Chinese Academy of Sciences, Shenyang 110016, People's Republic of China

E-mail: yangzq@imr.ac.cn

Received 8 June 2001
Published 30 August 2001
Online at stacks.iop.org/JPhysCM/13/8475

Abstract

The structural transition of the interphase boundary between crystalline Al and amorphous aluminium oxide under electron beam irradiation is investigated. Local amorphization took place on the crystalline Al side near the interphase boundary, when the current beam density was higher than 75 A cm^{-2} under electron beam irradiation. This was the result of mixing of oxygen into the crystalline Al, which resulted in formation of Al–O bonds. The amorphous Al_2O_3 irradiated by the electron beam was the main source of oxygen.

The effect of electron-beam (EB) irradiation on materials has been widely studied [1]. A high-energy (MeV) EB irradiation-induced crystal-to-amorphous (C–A) transition commonly occurred in some intermetallic compounds and ceramics [2, 3]. The energy transfers to the primary knock-on atoms are sufficient to produce only single or at most double atom displacement [4]. The displacement of the atoms forms lattice defects such as vacancies and interstitials. Through accumulation of the lattice defects, the irradiated crystal becomes disordered and rendered amorphous. Besides the amorphization, other phenomena were observed in some materials under EB irradiation, such as crystallization of pure germanium nanocrystals in amorphous Ge_XC_Y:H film [5], the tetragonal–orthorhombic phase transition in Fe-doped SnO_2 [6], and generation of small holes in MgO [7] and amorphous alumina [8]. Some noble metal particles a few nanometres in diameter became disordered during the EB irradiation. However, such disorder was in a dynamical state, i.e. the disordered particles could revert to crystalline again [9]. Usually, EB irradiation produced crystal defects, such as internal voids, planar defects, nanogrooves and nanoholes in pure metals [10]. For example, when aluminium foils were irradiated by EB, stacking faults were formed and they further evolved to stacking fault tetrahedra [11]. Well defined holes could be drilled in Al under the EB irradiation by sputtering of atoms

[1] Author to whom correspondence should be addressed.

0953-8984/01/378475+05$30.00

and vacancy enhanced displacement; no amorphization was observed before the generation of a hole [12]. Amorphization of Al has been reported by implanting Si or Ge into aluminium to form a supersaturated solid solution [13]. Aluminium oxide may be drilled when in contact with the aluminium substrate, which remains undrilled [14]. It can be seen that the effect of EB irradiation on materials is interesting and a rich literature has attested to the diversity of this field. However, most of them studied the bulk phase of materials; reports on the effect of EB irradiation on the interface (grain boundary or interphase boundary) are still limited [15]. In this letter, we will present our experiment on the local structural transition at the interphase boundary in an Al particle encapsulated by an amorphous Al_2O_3 shell under EB irradiation.

Irradiation experiments and *in situ* analysis were carried out in an HF2000 field emission gun transmission electron microscope (FEG TEM). This FEG TEM was operated at 200 kV and its vacuum was better than 2×10^{-6} Pa. An electron beam with the energy of 200 keV and beam current (I_P) of 5.4×10^{-10} A was available. The energy dispersive spectrum (EDS) analyser has an amorphous super-thin window, which can analyse light elements, such as O and N. The quantification was carried out by using Link ISIS software. The ultrafine Al particles were prepared by the active H_2 plasma evaporation method, and then passivated to form an oxide shell. Thin foils for TEM observation were prepared by Ar^+ ion milling of cold-compacted samples. In the irradiation experiment, the EB converged to less than 20 nm in diameter, and thus the beam-current density was higher than 160 A cm^{-2}.

Figure 1 shows successive stages of the local transition induced by EB irradiation at the interphase boundary of an Al/Al_2O_3 particle. Figure 1(a) demonstrates a typical morphology before irradiation, in which an Al particle is encapsulated by a 6 nm thick homogeneous shell. Figures 1(b) and (c) are the corresponding convergent beam electron diffraction (CBED) patterns for the core and shell, respectively. It is clear that the core is a perfect Al crystal and the shell is amorphous. If we converged EB to the interface region, both the Al crystal and amorphous Al_2O_3 were irradiated. After irradiation for about 300 s, the contrast of a small piece of Al under irradiation changed, as indicated by 'a' in figure 1(d). The corresponding CBED analysis proves that C–A transition has occurred in the irradiated Al region (figure 1(e)). If we focused the EB only on the newly formed amorphous region, a hole was drilled (figure 1(f)). Such a kind of irradiation-induced amorphization occurred commonly near the Al/Al_2O_3 interface. For example, another amorphous region (indicated by 'b' in figure 1(f)) could be produced by moving the EB to that region. However, if only a piece of pure Al region was irradiated, the C–A transition was never observed even when the irradiation time was prolonged. Therefore, the amorphous Al_2O_3 shell had an important effect on the amorphization of Al. Figure 2 shows the high-resolution electron microscopy image of the C–A transition region corresponding to figure 1(d), which indicates that the crystalline lattice of a piece of Al near the interface disappeared. It can be seen from figure 2 that local amorphization of Al at the interphase boundary was accompanied by a local thinning and cave-in of the amorphous shell.

In order to understand the role of oxygen in the C–A transition, EDS analysis was carried out during the whole process of irradiation. Figures 3(a), (b), (c) and (d) show compositions of the amorphous shell before and after irradiation, the newly formed amorphous region and the surrounding crystalline region, respectively. In comparison of figures 3(a) and (b), oxygen in the shell seems to decrease during the irradiation. In comparison of figures 3(c) and (d), some oxygen exists in the newly formed amorphous region, but not in the nearby Al region.

When amorphous alumina was irradiated by a high-energy EB above a critical current density, cations and anions could be separated to form O^{2-} noble gas bubbles [8]. According to this theory, some anions of O^{2-} might form in the amorphous Al_2O_3 shell under the EB irradiation. The flux of secondary electrons in the volume under the incident beam shows that the material in the centre of the irradiated area is positively charged with respect to the mean specimen

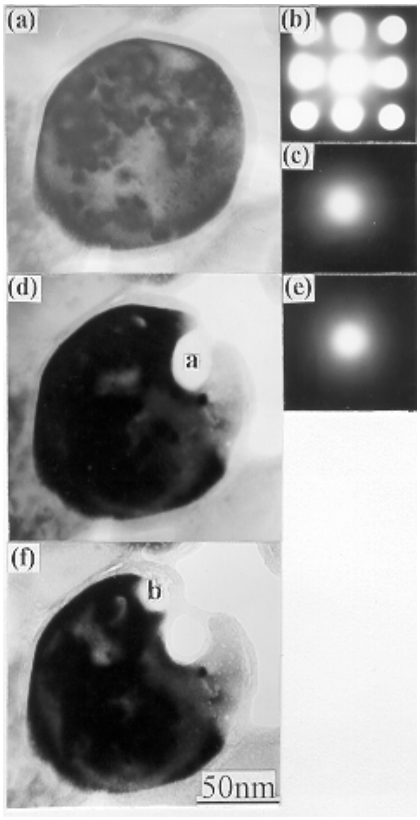

Figure 1. Successive stages of the boundary transition during the EB irradiation of an Al/Al_2O_3 particle. (a) Typical morphology before irradiation; (b) and (c) corresponding CBED patterns for the Al core and Al_2O_3 shell respectively; (d) a small amorphous region formed in the Al core; (e) the corresponding CBED pattern from region 'a'; (f) a hole was drilled in region 'a'.

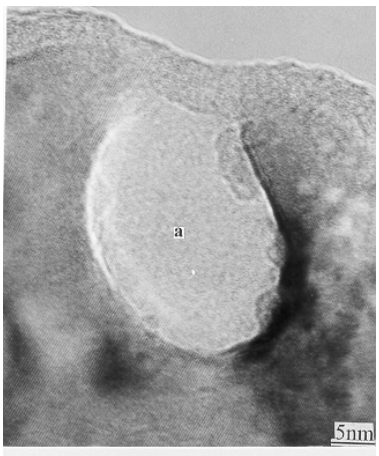

Figure 2. HREM image of the C–A transition region.

potential [8, 16, 17]. Therefore, it can be predicted that the free O^{2-} anions near the interface could diffuse into the Al crystal driven by the local electrostatic force. The mixing of oxygen into aluminium leads to the formation of Al–O bonds. This may be called oxidation, which results in amorphization of the irradiated Al. Oxidation-induced amorphization of Al has been observed by both experiments and molecular-dynamics simulation [18]. In addition, EB irradiation leads to a local temperature rise in the irradiated region [19]. However, the C–A transition

cannot occur if we move the EB to the pure Al region far from the Al/Al_2O_3 interface. It implies that such factors as the local temperature rise, the range of EB and energy density inside the irradiated cluster are not decisive in the C–A transition of Al. Therefore, the existence of the Al_2O_3 shell is necessary to provide oxygen for the C–A transition. The following hole-drilling occurred in the newly formed amorphous region in a manner similar to the process reported in [7] or [8]. After some oxygen anions near the interface diffused into the Al core, oxygen anions a little further from the interface would diffuse toward the interface. The diffusion process transported oxygen to the Al phase from the irradiated area of the oxide shell. As a result, the average composition of oxygen in the irradiated shell was decreased during irradiation.

From the EDS profiles (figures 3(a) and (b)), the Al/O ratio of the amorphous shell before and after irradiation can be quantified to be about 2:3 and 3:2, respectively. For simple consideration, the oxide shell changed from Al_2O_3 to Al_3O_2. This change can be expressed as $3Al_2O_3 \rightarrow 2Al_3O_2 + 5O$, i.e. every three Al_2O_3 molecules will lose five O atoms. From this model, 56% of the oxygen in the irradiated area of the shell was lost. Because the irradiated region was at the edge of the foil, it can be considered as homogeneous in thickness. The number of O atoms released from the irradiated shell can be evaluated by $n_O = 0.56 \times 3 \times N_a S_1 d\rho_1 / M_1$. $N_a S_1 d\rho_1 / M_1$ is the number of Al_2O_3 molecules in the irradiated shell, where N_a is the Avogadro number, S_1 is the irradiated area of the Al_2O_3 shell, d is the thickness, ρ_1 and M_1 are the density and molal weight of Al_2O_3, which are 3.9 g cm^{-3} and 102 g, respectively. In the same way, the Al atoms located originally in the converted region can be evaluated by $n_{Al} = N_a S_2 d\rho_2 / M_2$, where S_2 is the area of the newly formed amorphous region and ρ_2 (2.7 g cm^{-3}) and M_2 (27 g) are the density and molal weight of Al, respectively. Therefore, the atomic ratio of the Al atoms (in the EB irradiation-induced amorphous region) to the oxygen atoms (supplied by the oxide shell) can be evaluated by $f_{Al/O} = n_{Al}/n_o = 0.6 S_2 \rho_2 M_1 / S_1 \rho_1 M_2$. From figure 2, S_1 and S_2 can be measured to be about 80 nm^2 and 420 nm^2, respectively. Then $f_{Al/O}$ is about 8:1. From figure 3(c), this ratio can be experimentally measured to be 89:11. Repetition of EDS examination showed that the Al/O ratio ranged from 86:14 to 91:9 for the EB irradiation-induced amorphous region. The predicted value matches well with the experimentally obtained one. It should be noted that there is an error in the experimentally obtained Al/O ratio. Because the predicted Al/O ratio (8:1) is deduced based on the experimental data, there is an error similar to the experimental one in it. But the systematic error might be neglected, when comparing Al/O ratio obtained from different regions, if the experimental conditions were not remarkably changed. It is similar in cross-comparison between the experimental and theoretical Al/O ratio. Therefore, although the experimental values were not absolutely accurate, the matching between the predicted theoretical ratio of Al/O ratio (8:1) and the experimentally measured ratio (89:11) was probably not an occasional coincidence. There is little oxygen in the TEM column since the column vacuum is ultra-high ($<2 \times 10^{-6}$ Pa). In addition, irradiation of a pure Al region far from the interface did not result in amorphization, which also suggested that oxygen in the residual gases in the TEM could be neglected. Therefore, the matching between the theoretical and experimental values might qualitatively imply that the oxygen in the newly formed amorphous region was mainly provided by the oxide shell.

Our experiments also demonstrated that such local amorphization took place only after the incident EB was converged enough (<30 nm), namely the current density was high enough (>75 A cm^{-2}). The existence of a critical current density is consistent with other reports on defects induced by EB [8, 14]. The separation of cation and anion could occur only when the current density was higher than a threshold [8]. If the separation of cation and anion in the amorphous oxide shell did not occur, there would certainly no diffusion of oxygen from the oxide shell into the Al crystal. Because the crystalline Al and the amorphous oxide shell are side by side and the recoiling atoms have momentum in the direction of the incident

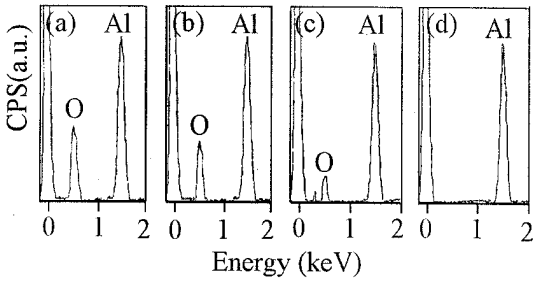

Figure 3. EDS results during the whole process of irradiation (a) and (b) for the amorphous shell before and after irradiation respectively, (c) and (d) for the newly formed amorphous region and nearby crystalline region respectively.

beam, simple recoil-implantation of oxygen sideways into the Al crystal is weak enough to be neglected. This is different from the case in Ge/Al or Si/Al bilayer specimens with an overlapping configuration under 1 MeV electron irradiation [13]. Therefore, there is a critical current density below which amorphization does not occur.

The EB irradiation caused diffusion of oxygen in the oxide shell into the Al phase at the interphase boundary. The mixing of oxygen into Al leads to the oxidation of Al, which results in the C–A transition in the irradiated area. Simply put, the C–A transition of pure aluminium under EB irradiation is a behaviour of oxidation. Although the local temperature rise induced by irradiation may influence the transition at the interphase boundary, it is not an essential prerequisite for the structural transition.

Acknowledgments

This work was supported by the National Natural Science Foundation of China under grants No 19874064 and No 59895156. The authors also appreciated Mr H T Cong and PhD student J Chen providing the Al/Al_2O_3 material.

References

[1] Mori H 1993 *Current Topics in Amorphous Materials: Physics and Technology* ed Y Sakurai *et al*, p 120
[2] Mori H, Fujita H, Tendo M and Fujita M 1984 *Scr. Metall.* **18** 783
[3] Inui H, Mori H and Fujita H 1990 *Phil. Mag.* B **61** 107
[4] Mori H and Fujita H 1982 *Japan. J. Appl. Phys.* **21** L494
[5] Tyczkowski J, Pietrzyk B, Mazurczyk R, Polanski K, Balcerski J and Delamar M 1997 *Appl. Phys. Lett.* **71** 2943
[6] Lu B, Wang C S and Zhang Y H 1997 *Appl. Phys. Lett.* **70** 717
[7] Turner P S, Bullough T J, Devenish R W, Maher S M and Humphreys C J 1990 *Phil. Mag. Lett.* **61** 181
[8] Berger S D, Salisbury I G, Milne R H, Imeson D and Humphreys C J 1987 *Phil. Mag.* B **55** 341
[9] Vanfleet R R and Mochel J 1996 *Microstructure Evolution During Irradiation, Symp. (Boston, MA, 1996)* p 685
[10] Griffiths M 1993 *J. Nucl. Mater.* **205** 225
[11] Furuya K, Piao M, Ishikawa N and Saito T 1996 *Microstructure Evolution During Irradiation, Symp. (Boston, MA, 1996)* p 331
[12] Humphreys C J, Bullough T J, Devenish R W, Maher D M and Turner P S 1990 *Scanning Micros.* **4** (Suppl.) 185
[13] Lin X W, Koike J, Seidman D N and Okamoto P R 1989 *Phil. Mag. Lett.* **60** 233
[14] Salisbury I G, Timsit R S, Berger S D and Humphreys C J 1984 *Appl. Phys. Lett.* **45** 1289
[15] Kizuka T, Iijima M and Tanaka N 1998 *Phil. Mag.* A **77** 413
[16] Varley J H 1962 *J. Phys. Chem. Solids* **23** 985
[17] Knotek M L and Feibelmen P J 1978 *Phys. Rev. Lett.* **40** 964
[18] Campbell T, Kalia R K, Nakano A, Vashishta P, Ogata S and Rodgers S 1999 *Phys. Rev. Lett.* **82** 4866
[19] Ba L, Qin Y and Wu Z 1996 *J. Appl. Phys.* **80** 6170